

3
4
5 **Could a future “Grand Solar Minimum” like the**
6 **Maunder Minimum stop global warming?**
7

8
9
10 Gerald A. Meehl^{1*}, Julie M. Arblaster^{1,2}, and Daniel R. Marsh¹
11

12
13 March 11, 2013
14

15
16
17 1) NCAR, P.O.Box 3000, Boulder CO 80307, (meehl@ucar.edu)

18 2) CAWCR, Melbourne, Australia

19 *NCAR is sponsored by the National Science Foundation
20

21 *Corresponding author, meehl@ucar.edu
22
23
24
25

26 Keywords: solar variability, Maunder Minimum, grand solar minimum, sun’s effects on earth’s
27 climate
28
29
30
31
32
33
34
35
36
37
38

Abstract

A future Maunder Minimum-type grand solar minimum, with total solar irradiance reduced by 0.25% over a 50 year period from 2020 to 2070, is imposed in a future climate change scenario experiment (RCP4.5) using, for the first time, a global coupled climate model that includes ozone chemistry and resolved stratospheric dynamics (WACCM). This model has been shown to simulate two amplifying mechanisms that produce regional signals of decadal climate variability comparable to observations, and thus is considered a credible tool to simulate the sun's effects on earth's climate. After the initial decrease of solar radiation in 2020, globally averaged surface air temperature cools relative to the reference simulation by up to several tenths of a degree Centigrade. By the end of the grand solar minimum in 2070, the warming nearly catches up to the reference simulation. Thus, a future grand solar minimum could slow down but not stop global warming.

1. Introduction

The Maunder Minimum in the late 17th Century was a roughly 50 year period from about 1650 to 1700 when sunspots vanished (Eddy, 1976), for reasons which are not yet fully understood (NRC, 2012). It is thought that the decrease in total solar irradiance (TSI) associated with the lower solar activity level contributed to the cooling evident over parts of the earth during the Little Ice Age (NRC, 2012). Since solar observations during the Maunder Minimum consist of records of sunspots, it is not entirely clear what the values of TSI were during that time. Recent studies have addressed aspects of this problem with more simplified models (e.g. Song et al., 2010, with a global atmospheric model coupled to a non-dynamic slab ocean; Feulner and

Rahmstorf, 2010, with an Earth System Model of Intermediate Complexity (EMIC); Jones et al., 2012, with a box diffusion energy balance model). All used values of TSI that ranged between reductions of roughly 0.01% and 0.25%. Earlier studies raised this issue as well (Wigley and Kelly, 1990; Thomas and Weiss, 2008). All have suggested the impact on globally averaged surface temperatures would be on the order of only several tenths of a degree C.

Since its cause is unknown, it is possible that the sun could go into another Maunder Minimum-type period of few sunspots and decreased TSI at any time. The question is, if that happened, could we better quantify whether the presumed cooling from a decrease of TSI would be enough to counteract human-caused warming? Here we address that question by introducing a Maunder Minimum-type grand solar minimum into a future climate simulation for the first time using a global coupled climate model with a resolved stratosphere and prognostic ozone chemistry.

2. Model and experiments

The climate model we use here is the Community Earth System Model using the Whole Atmosphere Community Climate Model version 4 as the atmospheric component called CESM1(WACCM). For a full description see Marsh et al. (2013). CESM1(WACCM) includes a “high top” atmospheric model, WACCM4, which is an extended version of the Community Atmospheric Model version 4 (CAM4) described by Neale et al. (2012). CAM4 was included in the Community Climate System Model version 4 (CCSM4; Gent et al., 2011). The WACCM4 has 66 vertical levels extending up to a height of approximately 140 km, a horizontal resolution of 1.9° latitude by 2.5° longitude, and includes ozone chemistry and wavelength dependence of

solar absorption. The ocean is a version of the Parallel Ocean Program (POP) with a nominal latitude-longitude resolution of 1° (down to $1/4^\circ$ in latitude in the equatorial tropics) and 60 levels in the vertical. Specifically, grid points in the ocean have a uniform 1.11° spacing in the zonal direction, and 0.27° near the equator, extending to 0.54° poleward of 35° N and S (Gent et al., 2011).

A previous version of WACCM was shown to be able to simulate two mechanisms that amplify relatively small fluctuations of TSI to produce measurable regional climate anomalies, though globally averaged response remained relatively small. The first is the “top-down” stratospheric ozone mechanism (e.g. Haigh, 2006; Balachandran et al, 1999; Shindell et al., 1999; Koder and Kuroda, 2002; Matthes et al., 2006), and the second is the “bottom-up” coupled air-sea mechanism (Meehl et al., 2008; Bal et al., 2011). Though not explicitly described or understood, elements of the bottom-up mechanism produced climate system responses in even very early global coupled climate models studies where the TSI was increased to produce increases of globally averaged temperature and associated changes in clouds (e.g. Wetherald and Manabe, 1986). Kristjansson et al. (2002) noted an association between solar variability and cloud cover in observations, and speculated that there could be an amplifying mechanism involving positive TSI, a slight warming of SSTs, and small reductions of low cloud cover. Though Cubasch et al. (1997) showed spatial patterns of the response to solar and greenhouse gases in a climate model simulation that were similar, Meehl et al. (2003) noted key differences in the SST patterns between CO_2 and solar forcing, with the latter having a La Niña-like pattern, and described the details of the coupled feedbacks involved with a bottom-up mechanism that would amplify the small solar forcing and involve cloud feedbacks. This amplifying mechanism

was then further quantified and modeled by Meehl et al. (2008). Meanwhile, Boer et al. (2005) studied the climate response to increased solar forcing, and Mann et al. (2009), in a paleoclimate context for the Medieval Climate Anomaly (MCA), noted the role of increased solar forcing in producing a tropical SST pattern not unlike that described in Meehl et al. (2003), along with a possible positive phase of the North Atlantic Oscillation (NAO). A number of these aspects were reviewed in the IPCC Fourth Assessment Report (Forster et al., 2007; Hegerl et al., 2007), though the amplification of regional signals by either the bottom-up or top-down mechanism was not considered. Since WACCM includes the processes essential to the bottom-up and top-down mechanisms, it is able to produce decadal variability of regional climate anomalies in the Indo-Pacific region (Meehl et al., 2009) that resemble those observed (e.g. van Loon et al., 2007) in both magnitude and regional pattern.

Various estimates have been made regarding how much lower than present-day were the Maunder Minimum values of TSI. These range from somewhere close to present solar minima (Schrijver et al., 2011), to a reduction of 0.15% to 0.3% below present solar minima (Foukal et al., 2011), to a reduction of more than 0.4% below present solar minima (Shapiro et al., 2011). Though the estimates for the greater reductions in TSI have been criticized as being too large (Feulner, 2011), for the purposes of this study we chose a reduction that is sufficiently large to produce a noticeable climate system response. The caveat for the present study is that an actual future Maunder Minimum-type event could feature a smaller reduction of TSI and an even lower climate system response. Thus for the present study, we use a reduction of 0.25% below recent measured solar minima to provide the model with a large but potentially feasible reduction of TSI that could have occurred during the Maunder Minimum.

132

133 The experiment is designed as follows and is illustrated in Fig. 1. Time-varying daily solar
134 spectral irradiances (SSI) are based on those used for the CESM1(WACCM) Coupled Model
135 Intercomparison Project Phase 5 (CMIP5) experiments. As described in Marsh et al. (2013),
136 these are specified from the model of Lean et al. (2005) and scaled by 0.9965 as recommended
137 by the CMIP5 protocol. For the RCP4.5 scenario, the 11-year solar cycle is included as a repeat
138 of the last four observed solar cycles, with 1965-2008 mapping onto 2009-2052 and 2053-2096
139 and so on. The grand solar minimum is computed as the average of the 1976, 1986 and 1996
140 solar minima multiplied by (1-0.0025) across all spectral irradiances. In the prescribed SSI
141 changes for these twentieth century minima, larger reductions (1-8%) occur in the ultraviolet
142 range than other parts of the spectrum and this is therefore also reflected in the grand solar
143 minima. Some studies argue for an even greater reduction in the UV during the Maunder
144 Minimum (e.g. Krivova and Solanki, 2005) but given the debate regarding SSI variations in the
145 most recent solar minima (Haigh et al 2010; Lean and DeLand, 2012), we chose to apply the
146 percentage-wise reduction equally across all spectral irradiances. The SSI in the model ramps
147 down to the minimum value linearly over 5 years from 2020-2024 and then back up from 2065-
148 2070 to the original values, through the experiment end at 2080. This 40-year length period of
149 low solar irradiance is chosen to be similar to the period during the Maunder Minimum for which
150 few sunspots were observed (Eddy, 1976). Three ensemble members are performed and
151 compared to the three CESM1(WACCM) RCP4.5 CMIP5 experiments. These experiments are
152 available from 2006-2065 (with one member extending to 2100) and include a repeating 11-year
153 solar cycle extending into the future (Meehl et al., 2012). Statistical significance is determined as

the 5% significance level from a two-sided Student t-test. Uncertainty ranges are given as +/- one standard deviation.

Results

Figure 2 shows the time series of globally averaged surface air temperature for the reference RCP4.5 climate change experiments compared to the grand solar minimum experiment simulations. After the initial reduction in SSI starting in 2020, the rate of global warming decreases for about 20 years, with an ensemble mean trend over the period 2020 to 2040 of $0.10 \pm 0.05^\circ\text{C}$ per decade in the grand solar minimum experiment, compared to the ongoing warming trend in the RCP4.5 experiment over that time period of $0.18 \pm 0.05^\circ\text{C}/\text{decade}$. For the 10 year average from years 2026-2035 near the beginning of the grand solar minimum experiment, the global warming in the reference simulation compared to the 1986-2005 period is 0.80°C , compared to 0.64°C in the grand solar minimum experiment, for a reduction of 0.16°C or about 19%. There are mostly negative differences compared to the reference simulation (Fig. 3a), but there are small amplitude (and not statistically significant) positive SST anomalies over the eastern tropical Pacific in the initial period 2026-2035. This is the opposite to the negative SST anomalies seen in that region for an increase in TSI associated with the 11 year solar cycle in observations (van Loon et al., 2007) and WACCM (Meehl et al., 2009), and thus is qualitatively consistent with the two mechanisms in WACCM that respond to changes in TSI. The pattern of midlatitude surface temperature anomalies stretching from the North Pacific across North America to the Atlantic is associated with precipitation and convective heating

anomalies in the tropical Pacific that produce a Pacific-North America (PNA) midlatitude teleconnection pattern that is also the opposite to that forced by an increase in TSI in the 11 year solar cycle (Meehl et al., 2008). Additionally, in the grand solar minimum experiment there are relative decreases of south Asian monsoon precipitation up to 15% (not shown), consistent with paleo evidence from the Maunder Minimum (Ueberoi, 2012). This is opposite to the signal of increased solar forcing in the 11 year solar cycle that produces somewhat larger magnitude Indian monsoon precipitation (Kodera, 2004; van Loon and Meehl, 2012), and is again consistent with the effects of changes in solar forcing on earth's climate.

By 2040 the warming trend in the grand solar minimum experiments has increased, with a trend of $0.20 \pm 0.04^\circ\text{C}$ per decade from 2040 to 2060, compared to the reference warming trend over that time period of $0.18 \pm 0.05^\circ\text{C}$ per decade. Since the reduced TSI has delayed this warming, the grand solar minimum experiment remains cooler than the standard RCP4.5 experiment. The warming compared to the 1986-2005 reference period in the RCP4.5 simulations is $0.98 \pm 0.05^\circ\text{C}$, compared to $0.74 \pm 0.05^\circ\text{C}$ in the grand solar minimum experiment, with the latter being relatively cooler by $0.24 \pm 0.05^\circ\text{C}$ for about 24% less warming from 2036 to 2045. This agrees well with the results of Feulner and Rahmstorf (2010) who find a reduction of 0.26°C for a similar forcing scenario in a simple model. In the global coupled model used here, the initial positive SST anomalies in the eastern tropical Pacific have transitioned to negative anomalies by this time (Fig. 3b) to join most of the tropical oceans with significantly cooler SSTs compared to the reference experiment, consistent with the opposite response to increased solar forcing that is evidenced by a transition of negative to positive SST anomalies in that region (Meehl and Arblaster, 2009). The relatively cooler conditions in the grand solar minimum experiment

remain for the 2046 to 2065 period, with global warming values of $1.27 \pm 0.05^\circ\text{C}$ in the RCP4.5 experiment, and $1.01 \pm 0.05^\circ\text{C}$ in the grand solar minimum experiment, a difference of -0.26°C or about 20% less warming. There are mostly cooler surface temperatures over the global tropics and areas of the high latitudes as well (Fig. 3c). However, as the grand solar minimum ends in 2065, temperatures begin to warm up again. Within the range of the natural variability in the different ensemble members, the grand solar minimum temperatures nearly approach values in the reference experiment as temperatures in the RCP4.5 experiment begin to level off as concentrations of greenhouse gases also level off as prescribed by the RCP4.5 mitigation scenario (Meehl et al., 2012). The warming trend from 2065 to 2080 is $0.11 \pm 0.11^\circ\text{C}$ per decade in RCP4.5, with a global warming value of $1.47 \pm 0.05^\circ\text{C}$, while the value for the grand solar minimum experiment for that time period is $0.13 \pm 0.06^\circ\text{C}$ per decade for a global warming value of $1.32 \pm 0.05^\circ\text{C}$.

A similar evolution occurs in the upper 300m ocean heat content (not shown), with initial decreases that then recover late in the experiment and approach the reference value by 2080. The mid-ocean layer (300m to 700m) however, stays cooler than the RCP4.5 reference experiment throughout the grand solar minimum experiment, while the deep ocean has very small amplitude changes.

Changes in zonal mean temperature (not shown) mostly reflect the surface temperature anomalies with cooling through most of the troposphere and stratosphere in the grand solar minimum experiment. This cooling throughout the atmosphere is consistent with previous studies of solar forcing which highlight the different fingerprint of solar (mostly uniform

temperature changes throughout the troposphere and stratosphere) to that of increased CO₂, the latter having a distinct pattern of warming in the troposphere and cooling in the stratosphere (Santer et al., 2003; Hegerl et al., 2007).

Thus, a grand solar minimum in the middle of the 21st Century would slow down human-caused global warming and reduce the relative increase of surface temperatures by several tenths of a degree. This confirms earlier results using simpler models. But when the TSI returns to the reference values, the system warms back up to approach the magnitude of the surface temperature anomalies in the reference RCP4.5 experiment. Therefore, results here indicate that such a grand solar minimum would slow down and somewhat delay, but not stop, human-caused global warming.

Acknowledgements

The authors thank Peter Foukal, Mark Miesch, and Phil Judge for very helpful consultations on the possible effect of the Maunder Minimum on TSI, Georg Feulner and one anonymous reviewer for constructive comments, Mike Mills for running the RCP4.5 experiment, and Hanli Liu, Lorenzo Polvani and the CESM Whole Atmosphere Working Group for their work in developing WACCM4. This research used computing resources of the Climate Simulation Laboratory at the National Center for Atmospheric Research (NCAR), which is sponsored by the National Science Foundation; the Oak Ridge Leadership Computing Facility, which is supported by the Office of Science of the U.S. Department of Energy and the National Energy Research Scientific Computing Center, which is supported by the Office of Science of the U.S. Department of Energy under Contract DEAC02-05CH11231. We acknowledge Adrienne

Middleton and Gary Strand for help with the model runs. Portions of this study were supported by the Office of Science (BER), U.S. Department of Energy, and the National Science Foundation. The National Center for Atmospheric Research is sponsored by the National Science Foundation.

References

Bal, S., S. Schimanke, T. Spanghel, and U. Cubasch (2011), On the robustness of the solar cycle signal in the Pacific region. *Geophys. Res. Lett.*, 38, L14809, doi:10.1029/2011GL047964.

Balachandran, N., D. Rind, P. Lonergan, D. Shindell (1999), Effects of solar cycle variability on the lower stratosphere and the troposphere. *J. Geophys. Res.*, 104, D22, doi:10.1029/1999JD900924.

Boer, G.J., K. Hamilton, and W. Shu (2005), Climate sensitivity and climate change under strong forcing. *Clim. Dyn.*, 24, 685—700, doi:10.1007/s00382-004-0500-3.

Cubasch, U., and co-authors (1997), Simulation of the influence of solar radiation variations on the global climate with an ocean-atmosphere general circulation model. *Clim. Dyn.*, 13, 757—767.

266 Eddy, J. A. (1976), The Maunder Minimum, *Science*, 192, 1189–1202.

267

268 Feulner, G. (2011), Are the most recent estimates for Maunder Minimum solar irradiance in
 269 agreement with temperature reconstructions?, *Geophys. Res. Lett.*, 38, L16706,
 270 doi:10.1029/2011GL048529.

271

272 Feulner, G., and S. Rahmstorf (2010), On the effect of a new grand minimum of solar activity on
 273 the future climate on Earth, *Geophys. Res. Lett.*, 37, L05707, doi:10.1029/2010GL042710.

274

275 Forster, P., and co-authors (2007), Changes in atmospheric constituents and in radiative forcing.
 276 In: S. Solomon et al. (ed.) Climate Change 2007. The Fourth Scientific Assessment,
 277 Intergovernmental Panel on Climate Change (IPCC), Cambridge University Press, Cambridge,
 278 129—234.

279

280 Foukal, P., A. Ortiz, and R. Schnerr (2011), Dimming of the 17th century sun. *Astrophys. J.*
 281 *Lett.* 733:L38, doi:10.1088/2041-8205/733/2/L38.

282

283 Gent, P. and coauthors (2011), The Community Climate System Model Version 4.
 284 *J. Climate*, 24, 4973-4991, doi: /10.1175/2011JCLI4083.1.

285

286 Haigh, J.D. (1996), The impact of solar variability on climate. *Science*, 272, 981—984.

287

288 Haigh, J.D., A. R. Winning, R. Toumi, and J. W. Harder (2010), An influence of solar spectral
289 variations on radiative forcing of climate. *Nature*, 467, 696–699
290

291 Hegerl, G. C., and co-authors (2007), Understanding and Attributing Climate Change. In: S.
292 Solomon et al. (ed.) Climate Change 2007. The Fourth Scientific Assessment, Intergovernmental
293 Panel on Climate Change (IPCC), Cambridge University Press, Cambridge, 663-745.
294

295 Jones, G. S., M. Lockwood, and P. A. Stott (2012), What influence will future solar activity
296 changes over the 21st century have on projected global near-surface temperature changes?,
297 *J. Geophys. Res.*, 117, D05103, doi:10.1029/2011JD017013.
298

299 Kodera, K. (2004), Solar influence on the Indian Ocean monsoon through dynamical processes.
300 *Geophys. Res. Lett.*, 31, L24209, doi:10.1029/2004GL020928.
301

302 Kodera, K., and Y. Kuroda (2002), Dynamical response to the solar cycle. *J. Geophys. Res.*,
303 107, 4749, doi:10.1029/2002JD002224.
304

305 Kristjansson, J.E. and co-authors (2002), A new look at possible connections between solar
306 activity, clouds and climate. *Geophys. Res. Lett.*, 29, doi:10.1029/2002GL015646.
307

308 Krivova, N.A., and S.K. Solanki (2005), Reconstruction of solar UV irradiance. *Adv. Sp. Res.*,
309 35, 361-364

310

311 Lean, J.L. and M.T. DeLand (2012), How does the sun's spectrum vary? *J. Climate*, 25, 2555–
312 2560, doi: <http://dx.doi.org/10.1175/JCLI-D-11-00571.1>.

313

314 Mann, M.E., and co-authors (2009), Global signatures and dynamical origins of the Little Ice
315 Age and Medieval Climate Anomaly. *Science*, 326, 1256—1260.

316

317 Marsh, D. R., M. J. Mills, D. E. Kinnison, J. -F. Lamarque, N. Calvo, and L. M. Polvani (2013),
318 Climate change from 1850 to 2005 simulated in CESM1(WACCM), *J. Climate*, submitted.

319

320 Matthes, K., Y. Kuroda, K. Loder, and U. Langematz (2006), Transfer of the solar signal from
321 the stratosphere to the troposphere: Northern winter. *J. Geophys. Res.*, 111, D06108,
322 doi:10.1029/2005JD006283.

323

324 Meehl, G.A., W.M. Washington, T.M. L. Wigley, J. M. Arblaster, and A. Dai (2003), Solar and
325 greenhouse gas forcing and climate response in the 20th century. *J. Climate*, 16, 426–444.

326

327 Meehl, G.A., and J.M. Arblaster (2009), A lagged warm event-like response to peaks in solar
 328 forcing in the Pacific region. *J. Climate*, 22, 3647--3660.

329

330 Meehl, G.A., J.M. Arblaster,, G. Branstator, and H. van Loon (2008), A coupled air-sea
 331 response mechanism to solar forcing in the Pacific region. *J. Climate*, 21, 2883—2897.

332

333 Meehl, G.A., J.M. Arblaster, K. Matthes, F. Sassi, and H. van Loon (2009), Amplifying the
 334 Pacific Climate System Response to a Small 11-Year Solar Cycle Forcing. *Science*, 325, 1114-
 335 1118.

336

337 Meehl, G.A., W.M. Washington, J.M. Arblaster, A. Hu, H. Teng, C. Tebaldi, B. Sanderson, J.F.
 338 Lamarque, A. Conley, W.G. Strand, and J.B. White III (2012), Climate system response to
 339 external forcings and climate change projections in CCSM4. *J. Climate*, 25, 3661—3683, doi:
 340 <http://dx.doi.org/10.1175/JCLI-D-11-00240.1>.

341

342 Neale, R. B., J. Richter, S. Park, P. H. Lauritzen, S. J. Vavrus, P. J. Rasch, and M. Zhang (2012),
 343 The Mean Climate of the Community Atmosphere Model (CAM4) in Forced SST and Fully
 344 Coupled Experiments. *J. Climate*, doi: <http://dx.doi.org/10.1175/JCLI-D-12-00236.1>.

345

346 NRC, National Research Council (2012), The Effects of Solar Variability on Earth’s Climate: A
 347 Workshop Report. The National Academies Press, Washington, D.C., U.S.A., www.nap.edu.

348

349 Uberoi, C. (2012), Little Ice Age in Mughal India: Solar minima linked to droughts? *EOS*, 93,

350 437-438.

351

352 Santer B.D., and co-authors (2003), Contributions of anthropogenic and natural forcing to recent

353 to recent tropopause height changes. *Science* , 301, 479-483.

354

355 Schrijver, C.J., W.C. Livingston, T.N. Woods, and R.A. Mewaldt (2011), The minimal solar

356 activity in 2008-2009 and its implications for long-term climate modeling. *Geophys. Res. Lett.*,

357 38, L06701, doi:10.1029/2011GL046658.

358

359 Shapiro, A.I., and co-authors (2011), A new approach to the long-term reconstruction of the solar

360 irradiance leads to large historical solar forcing. *Astron. Astrophys.*, 529, A67,

361 doi:10.1051/0004-6361/201016173.

362

363 Shindell, D., D.Rind, N. Balachandran, J. Lean, and J. Lonergan (1999), Solar cycle variability,

364 ozone, and climate. *Science*, 284, 305—308.

365

366 Song, X., D. Lubin, and G. J. Zhang (2010), Increased greenhouse gases enhance regional

367 climate response to a Maunder Minimum, *Geophys. Res. Lett.*, 37, L01703,

368 doi:10.1029/2009GL041290.

369

Thomas, J.H. and N.O. Weiss (2008), Sunspots and Starspots, Cambridge Astrophysics No. 46, Cambridge University Press, ISBN:9780521860031, 296pp.

van Loon, H., G.A. Meehl, and D.J. Shea (2007), Coupled air-sea response to solar forcing in the Pacific region during northern winter. *J.Geophys.Res.*, *112*, D02108, doi:10.1029/2006JD007378.

van Loon, H., and G.A. Meehl (2012), The Indian summer monsoon during peaks in the 11 year sunspot cycle. *Geophys. Res. Lett.*, *39*, L13701, doi:10.1029/2012GL051977.

Wetherald, R.T., and S. Manabe (1986), An investigation of cloud cover change in response to thermal forcing. *Clim. Change*, *8*, 5—23.

Wigley, T.M.L., and P.M. Kelly (1990), Holocene climatic change, 14C wiggles and variations in solar irradiance. *Philos. Trans. R. Soc. A*, *330*, 547—558.

Figure captions

Fig. 1: Time series of total solar irradiance input to WACCM showing a reduction of TSI from 2020 to 2070 of 0.25%.

Fig. 2: Time series of globally averaged surface air temperature anomalies (°C) relative to the 1986-2005 reference period for the WACCM standard RCP4.5 simulations (orange lines) and the

grand solar minimum experiment (blue lines). The duration of the grand solar minimum experiment shown in Fig. 1 is indicated from 2020-2070.

Fig. 3: a) Ensemble mean surface air temperature differences, grand solar minimum experiment minus reference RCP4.5 experiment, for the initial period after TSI is reduced (2026-2035), b) same as (a) except for near the middle of the grand solar minimum (2036-2045), and c) same as (a) except for a period near the end of the grand solar minimum (2046-2065). Globally averaged temperature anomalies are shown at upper left of each panel.

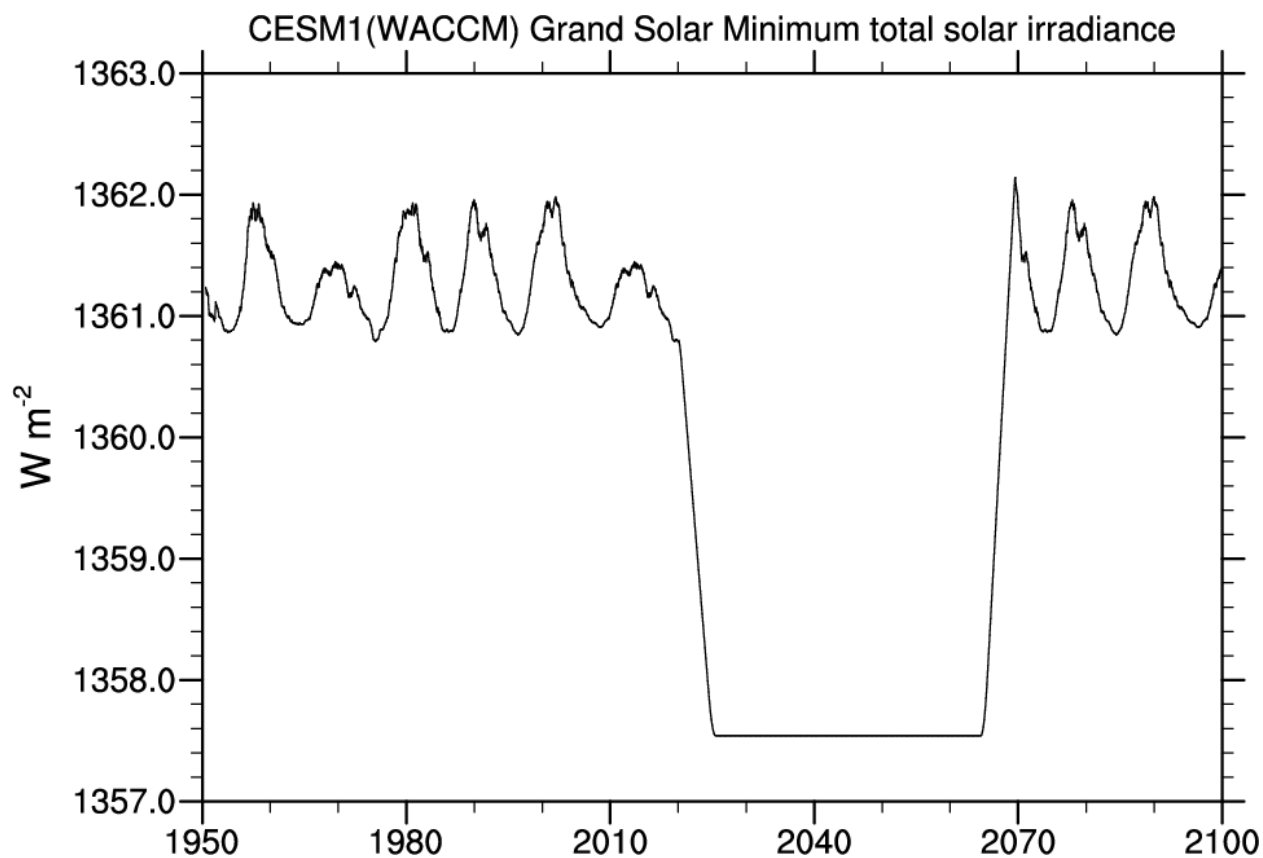


Fig. 1: Time series of total solar irradiance input to CESM1(WACCM) showing a reduction of TSI from 2025 to 2065 of 0.25%.

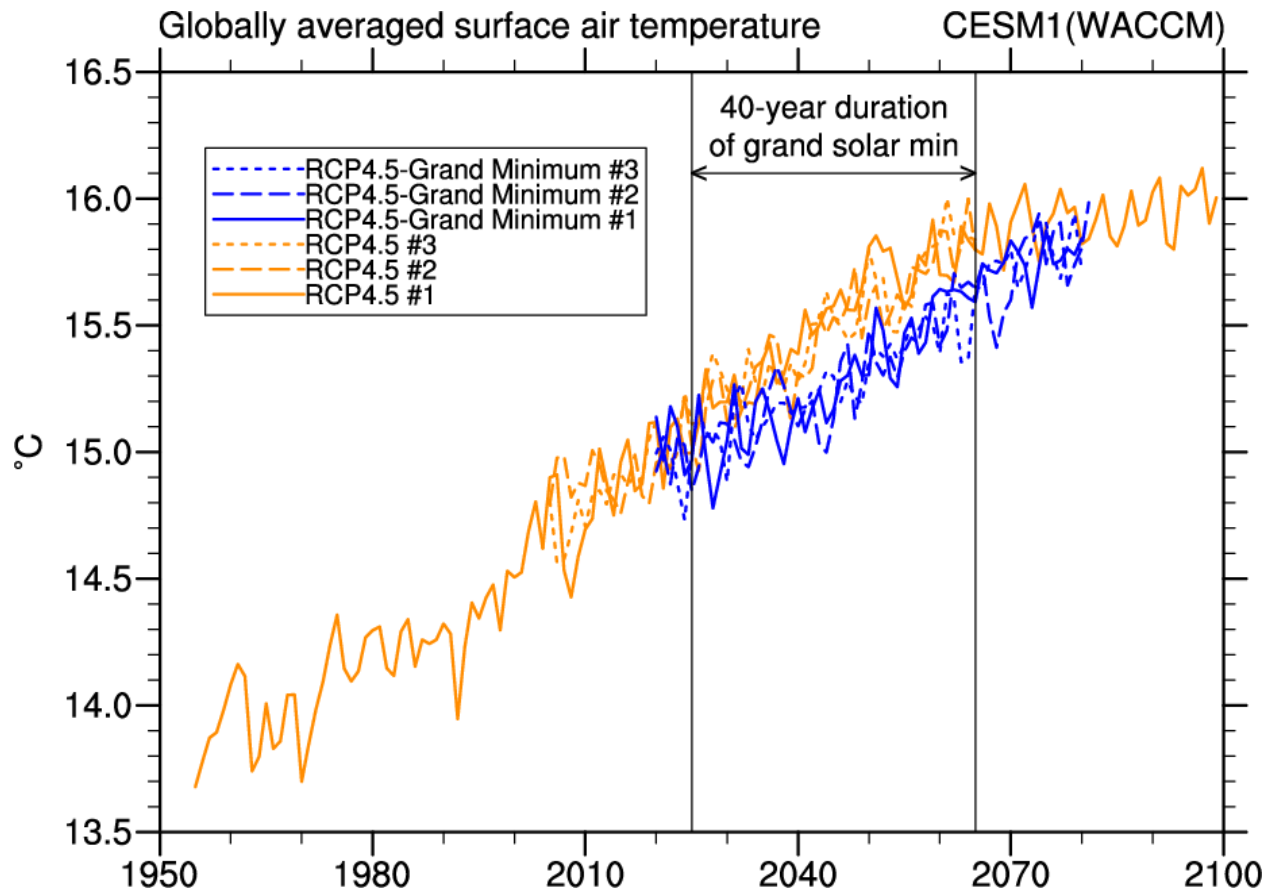
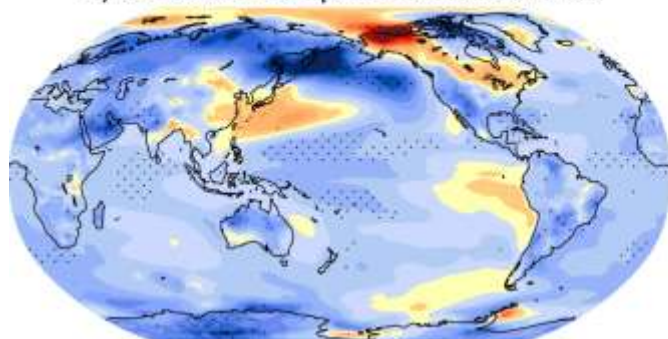


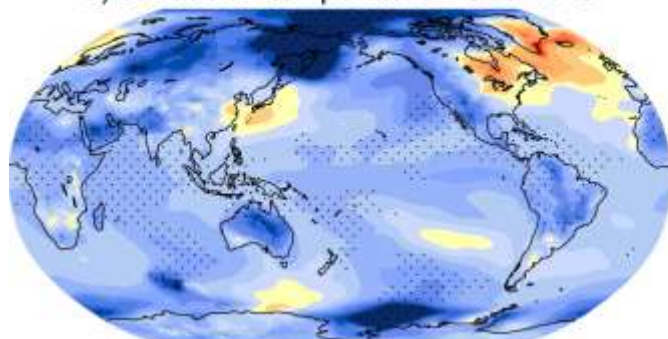
Fig. 2: Time series of globally averaged surface air temperature anomalies (°C) relative to the 1986-2005 reference period for the CESM1(WACCM) standard RCP4.5 simulations (orange lines) and the grand solar minimum experiment (blue lines). The duration of the grand solar minimum experiment shown in Fig. 1 is indicated from 2025-2065.

CESM1(WACCM) RCP4.5 Grand Solar Minimum difference

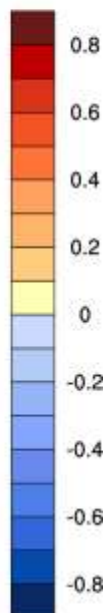
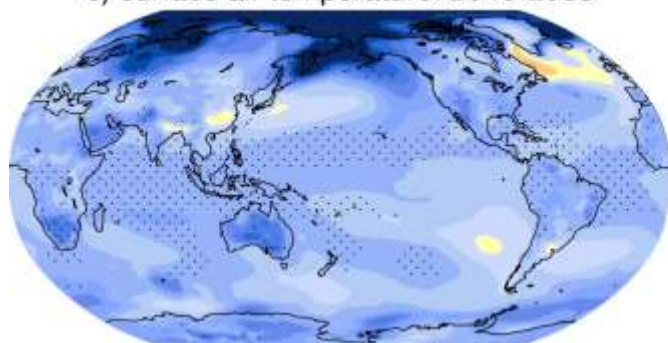
a) surface air temperature: 2026-2035



b) surface air temperature: 2036-2045

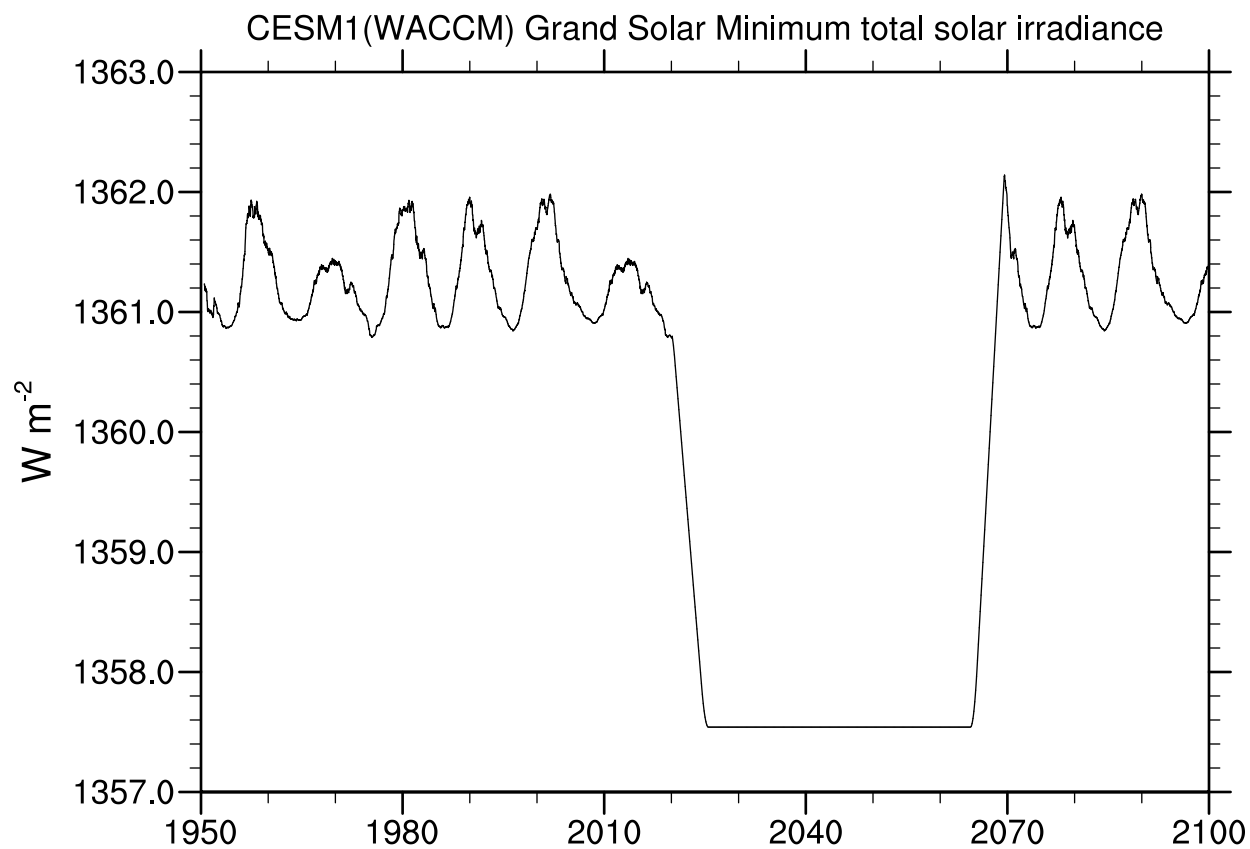


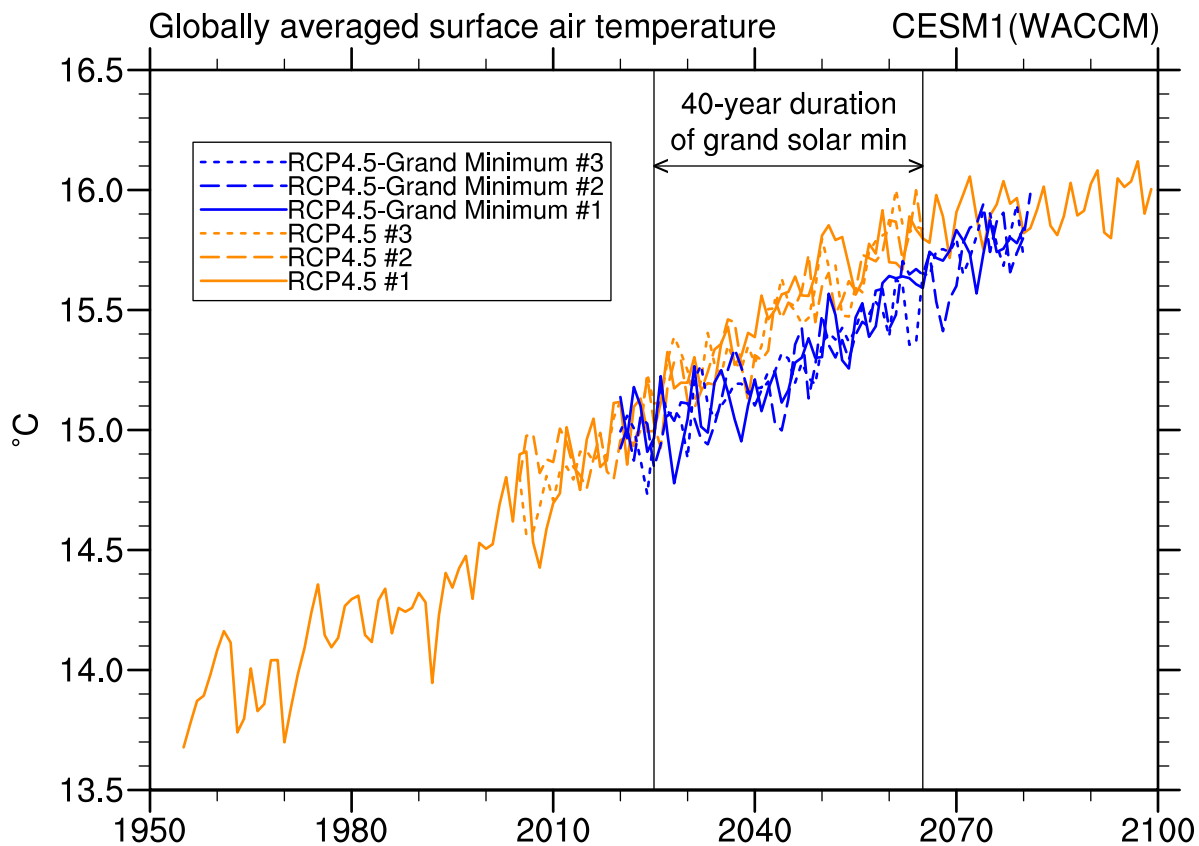
c) surface air temperature: 2046-2065



(°C)

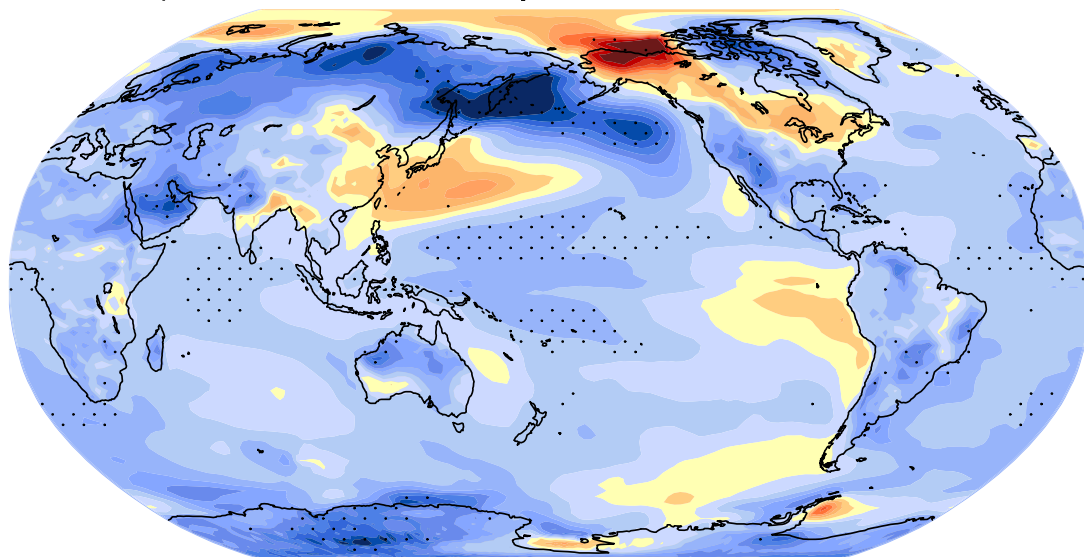
Fig. 3: a) Ensemble mean surface air temperature differences, grand solar minimum experiment minus reference RCP4.5 experiment, for the initial period after irradiances are reduced (2026-2035), b) same as (a) except for near the middle of the grand solar minimum (2036-2045), and c) same as (a) except for a period near the end of the grand solar minimum (2046-2065). Stippling indicates gridpoints where the difference is significant at the 95% level.



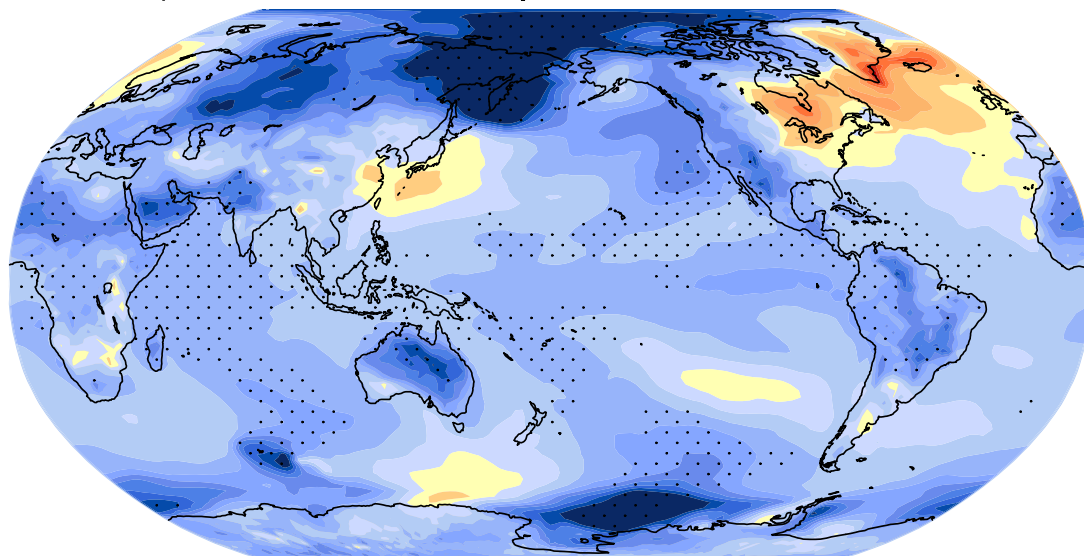


CESM1(WACCM) RCP4.5 Grand Solar Minimum difference

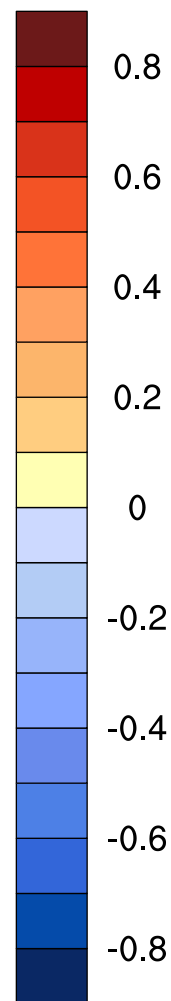
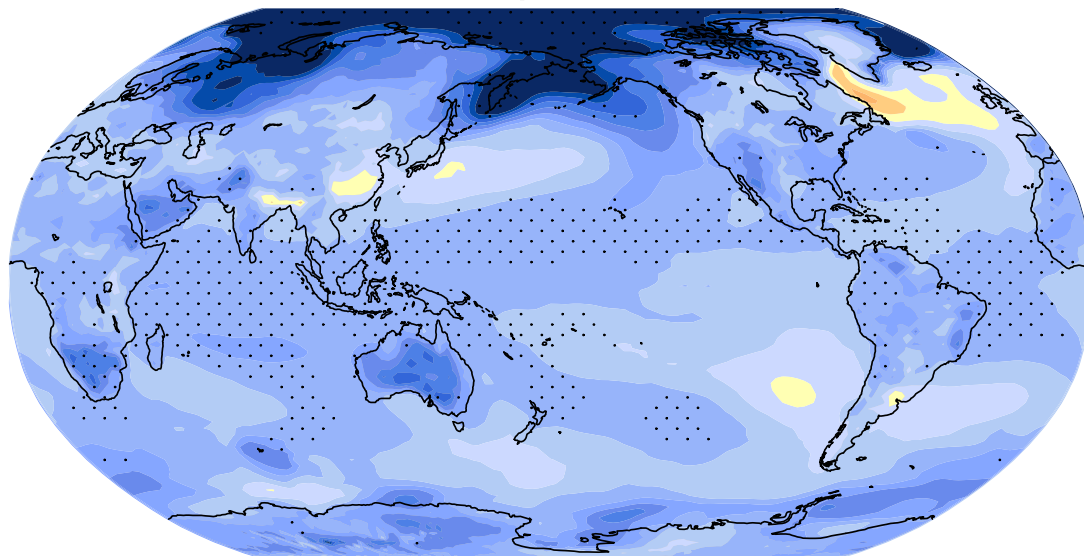
a) surface air temperature: 2026-2035



b) surface air temperature: 2036-2045



c) surface air temperature: 2046-2065



(°C)